

# Variational Approach to Real-Time Evolution of Yang-Mills Gauge Fields on the Lattice

C. Gong and B. Müller

Physics Department, P. O. Box 90305, Duke University  
Durham, NC 27708-0305, U.S.A.

and

T. S. Biró

Institut für Theoretische Physik

Justus-Liebig-Universität

Heinrich-Buff-Ring 16, D-6300 Giessen, Germany

May 3, 2019

## Abstract

Applying a variational method to a Gaussian wave ansatz, we have derived a set of semi-classical evolution equations for SU(2) lattice gauge fields, which take the classical form in the limit of a vanishing width of the Gaussian wave packet. These equations are used to study the quantum effects on the classical evolutions of the lattice gauge fields.

# 1 Introduction

Chaotic behavior in non-abelian gauge fields is first shown for the spatially homogenous potential configurations [1] and later also for the spherically symmetric fields [2]. Recently a real time evolution method is introduced to study general non-abelian gauge fields on a 3 dimensional lattice, where chaoticity is shown by obtaining a positive maximal Lyapunov exponent [3]. The maximal Lyapunov exponent is found to be related to the damping rate of gluons at rest, an infrared property of the quantized system. It can be argued that in the high temperature limit the properties associated with the infrared degrees of freedom in the gauge system are classical at the leading order. But it is still reasonable to ask how reliable these classical results are and what kind of effects the quantum corrections might bring about.

A classical dynamical system can be studied in two ways. One is by tracing single particle trajectories using Newton's equation. The other is by studying the phase space density evolution based on Liouville's equation. The links between classical and quantum physics have been studied in both formalisms for a long time. One of these links is the Wigner function which is the counterpart of the phase space distribution in classical dynamics [4]. The driving force of its evolution can be separated into classical and quantum parts [6]. Unfortunately the variables in the lattice gauge theory are defined on a compact group manifold with a non-trivial geometry. The Wigner function on a compact position space is defined on a discrete momentum space [5], rendering the classical limit rather subtle. Therefore we want to explore a more direct analogy to a classical trajectory in quantum physics, namely the evolution of a narrow wave packet. In order to resemble a classical trajectory as close as possible, the width of the wave packet in coordinate space and that in momentum space shall satisfy the uncertainty relation most efficiently, which suggests that we shall choose a Gaussian.

In this paper, as our first attack on the problem of quantum effects on the classical evolution of a gauge system, we apply the variational method to Gaussian wave packets [7, 8]. The basic idea is to parametrize a wave packet, usually a Gaussian one, by a small number of parameters. Then the time dependent variational principle is used to derive a set of evolution equations for these parameters, which have a symplectic structure like Hamiltonian equations. If the parameters are chosen in such a way that some of them resemble the variables in the corresponding classical system, then the coupling between the semi-classical time evolution of these parameters and that of all others can be interpreted as quantum corrections to the classical evolution. This method has been used to treat the scattering problem of  $\alpha$  particles [9], and recently it also has been applied to the many body problem of interacting fermion systems [10, 11]. In the following we will first introduce the method. Then it will be applied to the pure SU(2) lattice gauge system. The semi-classical Hamiltonian and the equations of motion will be derived and their solutions will be studied numerically.

## 2 Method

We begin by considering a quantum system described by a Hamiltonian  $H$ . The dynamics of the system is contained in the Schrödinger equation

$$i\hbar\partial_t|\Phi(t)\rangle = H|\Phi(t)\rangle. \quad (1)$$

We solve this equation by the time-dependent variational method [8] as follows. A normalized trial wavefunction  $|\Phi(q)\rangle$ , where  $q$  denotes a set of variational parameters, must satisfy the following variational principle

$$\delta \int_{t_1}^{t_2} dt \langle \Phi(q(t)) | (i\hbar\partial_t - H) | \Phi(q(t)) \rangle = 0. \quad (2)$$

Among these parameters some have definite meanings in the classical limit, such as the classical momenta and positions. Provided that enough parameters are chosen to span the whole Hilbert space, (2) can solve (1) exactly. Another case, when this is possible, is if we choose the parameters so clever that the exact time evolution of the initial state admixes only states from that part of the Hilbert space which is spanned by these trial states. But generally (2) is only an approximation to (1). Performing the variation in the usual way we can derive an effective Lagrangian

$$L = \dot{q}_i z_i(q) - \mathcal{H}(q) \quad (3)$$

with

$$z_i(q) = \frac{i}{2} \left( \langle \Phi | \frac{\partial \Phi}{\partial q_i} \rangle - \langle \frac{\partial \Phi}{\partial q_i} | \Phi \rangle \right) \quad (4)$$

and

$$\mathcal{H}(q) = \langle \Phi | H | \Phi \rangle . \quad (5)$$

In the equations of motion,

$$A_{ij}(q) \dot{q}_j = \frac{\partial \mathcal{H}}{\partial q_i} , \quad (6)$$

the antisymmetric coefficient,

$$A_{ij}(q) = i \left( \frac{\partial}{\partial q'_i} \frac{\partial}{\partial q_j} - \frac{\partial}{\partial q_i} \frac{\partial}{\partial q'_j} \right) \ln \langle \Phi(q') | \Phi(q) \rangle \Big|_{q'=q} , \quad (7)$$

occurs, which satisfies the Jacobi identity as well,

$$\frac{\partial A_{ij}}{\partial q_k} + \text{cyclic permutations} = 0. \quad (8)$$

Since  $A_{ij}$  is antisymmetric, the expectation value of the energy,  $\mathcal{H}$ , is conserved,

$$\frac{d\mathcal{H}}{dt} = \dot{q}_i A_{ij} \dot{q}_j = 0. \quad (9)$$

Other conservation laws related to symmetries of the quantum system can be derived accordingly.

Suppose that  $G$  is a generator of an infinitesimal symmetry transformation related to a conserved charge, i.e. it commutes with the Hamilton operator

$$[H, G] = 0. \quad (10)$$

Denote the corresponding 'classical operator' by  $G_0$ , whose action on the respective classical parameter  $x_0$  is identical to that of the 'quantum operator'  $G$  on the variable  $x$

$$G : x \rightarrow f(x) \quad G_0 : x_0 \rightarrow f(x_0). \quad (11)$$

We call our trial wave function covariant under the transformation  $G$  if it is invariant under the joint operation of  $G$  and  $G_0$ ,

$$(G + G_0) | \Phi \rangle = 0. \quad (12)$$

Such wave functions lead to a conserved expectation value

$$\frac{d\mathcal{G}}{dt} = 0, \quad (13)$$

with

$$\mathcal{G} = \langle \Phi | G | \Phi \rangle . \quad (14)$$

To prove this, let us consider an infinitesimal symmetry transformation generated by  $G_0$ . From the variational principle (2), we have

$$\int dt (\langle \delta \Phi | (i\hbar \partial_t - H) | \Phi \rangle + \langle \Phi | (i\hbar \partial_t - H) | \delta \Phi \rangle) = 0, \quad (15)$$

with

$$|\delta \Phi \rangle = i\delta\alpha G_0 | \Phi \rangle$$

$$\langle \delta \Phi | = -i\delta\alpha \langle \Phi | G_0, \quad (16)$$

where  $\delta\alpha$  is a small *real* parameter.

The above integrand can be casted into the form

$$-\delta\dot{\alpha} \langle \Phi | G_0 | \Phi \rangle - \delta\alpha \langle \Phi | \dot{G}_0 | \Phi \rangle - i\delta\alpha \langle \Phi | [G_0, H] | \Phi \rangle. \quad (17)$$

Now using  $G_0 | \Phi \rangle = -G | \Phi \rangle$  the commutator term vanishes, because  $G$  commutes with  $H$ . The rest can be splitted into a total time derivative, which we ignore in the variational integral, and into terms proportional with  $\delta\alpha$ . Finally we get

$$\int dt \delta\alpha \left( \langle \dot{\Phi} | G_0 | \Phi \rangle + \langle \Phi | G_0 | \dot{\Phi} \rangle \right) = 0. \quad (18)$$

Using again  $G_0 | \Phi \rangle = -G | \Phi \rangle$  and the fact that  $\dot{G} = 0$ , we arrive at

$$-\int dt \delta\alpha \left( \langle \dot{\Phi} | G | \Phi \rangle + \langle \Phi | \dot{G} | \Phi \rangle + \langle \Phi | G | \dot{\Phi} \rangle \right) = 0, \quad (19)$$

which, for  $\delta\alpha$  being arbitrary, is equivalent to

$$\frac{d}{dt} \langle \Phi | G | \Phi \rangle = 0. \quad (20)$$

We intend to use this property of the time-dependent variational principle in the following in order to ensure that Gauss's Law is satisfied on the average during the time evolution of Yang-Mills systems.

### 3 SU(2) Lattice Gauge Theory

#### 3.1 Variational Wavefunctions

Now we apply this method to lattice gauge theory. Here we restrict ourselves to SU(2) theory for simplicity. The lattice gauge Hamiltonian is [12]

$$H = \frac{g^2}{a} \left( \sum_l \frac{1}{2} E_l^a E_l^a + \frac{4}{g^4} \text{Re} \sum_p \left( 1 - \frac{1}{2} \text{tr} U_p \right) \right), \quad (21)$$

where the first term corresponds to the electric and the second to the magnetic energy. In the classical limit the pure gauge theory is scale invariant. The coupling constant  $g^2$  and the lattice spacing  $a$  can be scaled out entirely and we are left with no free parameter except the total energy (or temperature). In the semiclassical approach we want to consider the quantum corrections to classical trajectories so Planck's constant  $\hbar$  comes in naturally. After making the following scaling transformation,

$$\begin{aligned} H' &= ag^2 H, \\ t' &= t/a, \\ E' &= g^2 E, \\ \hbar' &= g^2 \hbar, \end{aligned} \quad (22)$$

the variables on the left become dimensionless numbers. In the following all quantities are understood to be the scaled ones unless otherwise stated explicitly. The equations all stay the same except that we shall put  $a = 1$  and  $g = 1$ . The scaled parameter  $\hbar = 4\pi\alpha_s$ , where  $\alpha_s = g^2\hbar/4\pi$  is the dimensionless coupling constant in the gauge theory, enters our formalism in two ways. First it appears in the variational principle,

$$\delta \int_{t_1}^{t_2} \langle \Phi | (i\hbar\partial_t - H) | \Phi \rangle = 0. \quad (23)$$

Secondly it also enters the commutation relation,

$$[E_l^a, A_m^b] = -i\hbar\delta^{ab}\delta_{lm}. \quad (24)$$

The explicit appearance of coupling constant in our calculation fixes the scale of quantum effects relative to classical effects.

To proceed we need to choose a trial wavefunction. In the strong coupling and zero temperature limit, the ground state wave function is an expansion of plaquette variables  $tr U_p$  [12]. It is separable for different plaquettes, but this choice is not very practical in our context. First we want the trial function to have the feature that the averages can be performed in closed analytical expressions. A plaquette separable wavefunction is more difficult in this aspect than a link separable one (see below). The second reason is that we are mainly interested in the high temperature limit where the system can be treated classically. In this limit the former is not a priori better justified than the latter. Moreover, since in the classical limit we deal with link variables rather than plaquette variables, a link separable wavefunction allows to make a more direct connection to classical dynamics. We choose the following Gaussian ansatz,

$$\Phi[U_l] = \prod_l \phi_l(U_l) = \prod_l \frac{1}{\sqrt{N_l}} \exp\left(\frac{b_l}{2} \text{tr}(U_l U_{l0}^{-1}) - \frac{1}{\hbar} \text{tr}(E_{l0} U_l U_{l0}^{-1})\right). \quad (25)$$

The  $U_{l0}$  and  $E_{l0}$  are parameters of the wavefunction, which correspond to classical link variables and left electric fields, respectively. Physically they denote the center of the coordinates and momenta of the Gaussian wave function. The  $U_l$ 's and  $U_{l0}$ 's are group elements of  $SU(2)$ , whereas the  $E_{l0}$  are elements of the  $su(2)$  algebra. The complex parameter  $b = v + iw$  controls the width, or more explicitly,  $\sqrt{v}$  is the inverse of the width.  $N_l$  is a normalization constant to be specified later.

The form (25) is chosen so that it is covariant under the gauge transformations, i.e. invariant under the simultaneous gauge transformation on both the quantum variables  $U_l$  and the classical parameters  $U_{l0}$  and  $E_{l0}$ ,

$$U'_l = g_L U_l g_R^{-1} \quad U'_{l0} = g_L U_{l0} g_R^{-1} \quad \text{and} \quad E'_{l0} = g_L E_{l0} g_L^{-1}, \quad (26)$$

where  $g_{L(R)}$  is a gauge transformation at the site left(right) to the link  $l$ . This leads to the desirable result that Gauss's law is conserved on average.

We note here that color confinement requires that all physical states shall be color singlet, while the trial wavefunction we use here is not gauge invariant. Is this a contradiction? The answer is yes in the sense that our choice does not correspond directly to a physical state. But here we have two arguments to support our choice. First we note that a covariant description is as close as we can get in the classical limit where we are always using color octet variables  $U_l$  and  $E_l$  to define a gauge configuration. Had we started from a color singlet trial wavefunction and wanted to derive classical equations of motion for averages of these variables, we would always get vanishing expectation values because of the Wigner-Eckart theorem. The second argument is that given a gauge covariant wavefunction we can easily project out its singlet part. So the knowledge of the former can help to understand the properties of a gauge invariant state.

In the continuum limit, this wavefunction formally coincides with a Gaussian in the vector potential  $A(x)$ ,

$$\Phi[A(x)] = \frac{1}{\sqrt{N}} \exp\left[\int d^3x \sum_a \left(-\frac{b(x)}{8} (A^a(x) - A_0^a(x))^2 + \frac{i}{\hbar} E_0(x)^a A^a(x)\right)\right] \quad (27)$$

The wavefunction (25) is normalized on each link with

$$N(v) = 2\pi^2 I_1(2v)/v, \quad (28)$$

where  $I_n$  denotes the modified Bessel function. Wavefunctions with different parameters are not orthogonal to each other. They form a set of overcomplete basis states of the Hilbert space for each link, with the completeness relation

$$\int dU_0 d^3 E_0 \Phi(E_0, U_0, b) \Phi(E_0, U_0, b) = 1, \quad (29)$$

for arbitrary  $b$ . This permits us to deal with the complex width parameter  $b$  in two ways. We could define a measure  $\mu(b)$  which satisfies

$$\int d\mu(b) = 1, \quad (30)$$

so that we formally have complete closure relation over all parameters

$$\int dU_0 d^3 E_0 d\mu(b) \Phi(E_0, U_0, b) \Phi(E_0, U_0, b) = 1. \quad (31)$$

The exact form of  $\mu(b)$  is not known, but could be obtained with numerical techniques. On the other hand we can treat  $b$  as an additional variational parameter. We will adopt this point of view here.

The relation between our classical parameters and the averaged quantities are obtained as

$$\begin{aligned} \langle E^a \rangle &= f(v) E_0^a, \\ \langle E_R^a \rangle &= f(v) E_{R0}^a, \\ \langle U \rangle &= f(v) U_0, \end{aligned} \quad (32)$$

where  $E_R^a \tau^a = U \tau^b U^{-1} E^b$  are the so called right electric fields and the function,

$$f(v) = \frac{1}{2} \frac{\partial \ln N(v)}{\partial v} = \frac{I_2(2v)}{I_1(2v)} \rightarrow \begin{cases} (v/2)(1 - v^2/6) & v \ll 1 \\ 1 - 3/(4v) & v \gg 1 \end{cases} \quad (33)$$

is plotted in Fig.1 (solid line). Due to the combined effect of the curvature of the SU(2) group manifold and the finite width of the wave packet, the average of  $E$  and  $U$  are not just their corresponding classical parameters as we would expect for a Euclidean parameter space. In the small width limit, i.e.  $v \rightarrow \infty$ ,  $f(v)$  approaches unity, a manifestation that locally the group manifold has Euclidean metric. From this we already see that the non-trivial geometry plays an important role here. We may also study the quadratic fluctuations of  $U$  and  $E$ . We calculate

$$\langle E^2 \rangle = \sum_a \langle E^a E^a \rangle = \hbar^2 \frac{3f}{8v} (v^2 + w^2) + \left(1 - \frac{f}{2v}\right) E_0^2. \quad (34)$$

We shall later see that the ensemble average of  $v$  is proportional to  $\hbar^{-1}$  and ensemble average of  $w$  is zero for  $v \rightarrow \infty$ . So in the classical limit, i.e.  $\hbar \rightarrow 0$ ,  $\langle E^2 \rangle$  goes to the classical result  $E_0^2$ . The variance of electric fields is

$$(\Delta E)^2 \equiv \sum_a (\langle E^a E^a \rangle - \langle E^a \rangle^2) = \hbar^2 \frac{3f}{8v} (v^2 + w^2) + \left(1 - \frac{f}{2v} - f^2\right) E_0^2, \quad (35)$$

which goes to zero like  $\frac{3}{8} \hbar^2 v + \frac{E_0^2}{v}$  in the classical limit. The fluctuation of the vector potential  $A$  is

$$(\Delta A)^2 \equiv 8 \left(1 - \frac{1}{2} \text{tr}(U U_0^{-1})\right) = 8(1 - f). \quad (36)$$

It vanishes in the classical limit like  $\hbar$ . We can check the uncertainty relation  $\Delta E \Delta A \geq 3(\hbar/2)$ , which becomes an equality in the vacuum. i.e.  $T = 0$  or  $E_0 = 0$ . As we already said, Gauss's law is satisfied on average, but it is not conserved at the operator level. The magnitude of fluctuating color charge at each lattice site is measured by

$$(\Delta G)^2 \equiv \sum_a (\langle G^a G^a \rangle - \langle G^a \rangle^2), \quad (37)$$

where the second term vanishes. Inserting the expression of the generator of time independent gauge transformation,

$$G^a = \sum_{i=1}^3 (E^a(\mathbf{n}) - E_R^a(\mathbf{n} - \mathbf{e}_i)), \quad (38)$$

where the summation runs over the three positive directions at one site, and  $\mathbf{n}$  denotes the position of the site and  $\mathbf{e}_i$  is the unit vector in  $i$ th direction, we obtain

$$(\Delta G)^2 = \sum_{i=1}^6 (\Delta E)_i^2, \quad (39)$$

where the summation now runs over all the links joining at one site. Each link contributes its electric field fluctuation to the local charge fluctuation. The correlations between different links do not appear because we have chosen a link separable wavefunction.

### 3.2 Effective Hamiltonian

The complete expression for the average total energy is

$$\begin{aligned}
H_{sc} &= H_e + H_0 + H_m \equiv \langle H \rangle \\
&= \sum_l \left[ \frac{1}{2} \left( 1 - \frac{f_l}{2v_l} \right) E_{l0}^2 \right] + \sum_l \left[ \hbar^2 \frac{3f_l}{16v_l} (v_l^2 + w_l^2) \right] + \\
&\quad 4 \sum_p \left( 1 - \frac{1}{2} f_p \text{tr} U_{p0} \right),
\end{aligned} \tag{40}$$

where  $f_p$  is the product of  $f_l = f(v_l)$  of the four links that circumvent the plaquette  $p$ . This semi-classical Hamiltonian consists of three parts. First we have the modified electric energy ( $H_e$ ) and magnetic energy ( $H_m$ ), which result in a coupling between the  $U_l$ ,  $E_l$  and the width parameters  $v_l$  and  $w_l$ , and thus modify the classical evolution of  $U_l$  and  $E_l$ . These modifications contain both genuine quantum effects and lattice artifacts, which are difficult to separate. Besides the modified classical electric and magnetic energy there is a zero point energy ( $H_0$ ) which is a consequence of the uncertainty relation. It increases linearly with  $v$  in the limit of large  $v$ .

We can study thermodynamical properties of the system described by  $H_{sc}$ . Consider the system at equilibrium with temperature  $T$ . The integration measures of  $E$  and  $U$  are the same as in the classical case. The integration over  $E$  is plagued by Gauss's law which eliminates one third of the degrees of freedom. The average magnetic energy is complicated by the interactions between different links. They make it very difficult to obtain the exact solution analytically. In the rest of this subsection, let us simplify ourselves to consider the Hamiltonian of a single link and a single plaquette. In this free link and plaquette limit the partition function can be factorized into three parts,

$$Z_{sc} = Z_e Z_m Z_0, \tag{41}$$

with

$$\begin{aligned}
Z_e &= \left( \frac{T}{2 - f/v} \right)^{3/2}, \\
Z_m &= N(2f_p/T) \exp(-4/T), \\
Z_0 &= \exp(-H_0/T),
\end{aligned}$$

where the subscripts  $e, m, 0$  denote contributions from electric, magnetic and zero-point energy, respectively.  $N(x)$  is the normalization function defined in (28). From the partition function we can easily obtain the ensemble averaged energy

$$\begin{aligned}
\langle \langle H_e \rangle \rangle &= 3T/2, \\
\langle \langle H_m \rangle \rangle &= 4(1 - f_p f(2f_p/T)), \\
\langle \langle H_0 \rangle \rangle &= H_0,
\end{aligned} \tag{42}$$

where  $\langle \langle \dots \rangle \rangle$  denotes ensemble average. We see that the electric energy is the same as that in the classical limit. In the classical limit  $f_p = 1$  so  $\langle \langle H_m \rangle \rangle = 4(1 - f(2/T))$ . When  $T \ll 2$ ,  $\langle \langle H_m \rangle \rangle$  takes the correct classical limit  $3T/2$  as demanded by the equipartition theorem. At larger  $T$  the energy temperature relation is distorted by the compactness of the gauge group. The free energy  $F = -T \ln Z$  is obtained as

$$F(v) = \frac{3T}{2} \ln \left( \left( 2 - \frac{f}{v} \right) \frac{1}{T} \right) + \frac{3\hbar^2}{16} f v + 4 - T \ln N \left( \frac{2f_p}{T} \right). \tag{43}$$

To see how the free energy looks like, we plot this function at  $T = 0.5$  and at  $T = 0$  in Fig2. The two plots are very similar in shape, and both have a first order phase transition. At small  $\hbar$  the free energy has two minima, one of which is at  $v = 0$ . The second minimum can be obtained in the limit of large  $v$  by minimizing the free energy, and the result is

$$v = 2(16 - 7T)^{1/2}/\hbar. \tag{44}$$

When  $\hbar$  increases, this second minimum rises until it fails to be a minimum at a critical value of  $\hbar$ , where a first order transition occurs. The critical value increases with temperature. From the plots we see for  $T = 0$  it occurs at  $\hbar \approx 1.73$  (the short dashed line in Fig.2b) and  $\hbar \approx 3$  for  $T = 0.5$  (the long dashed line in Fig.2a). This indicates the underlying potential has a non-trivial structure. Vacuum energy is obtained from the free energy by setting  $T = 0$ ,

$$F_0 = \frac{3\hbar^2}{16}fv + 4(1 - f^4). \quad (45)$$

At large  $\hbar$ , we only have one minimum  $v = 0$ . The wavefunction is so broad that it covers the whole group manifold and we are in quantum physics region. The corresponding energy is 4 (or  $4/g^2a$  in original variables). This is coincident with the leading order result of a perturbative calculation in the strong coupling limit [12]. In the other limit,  $\hbar \rightarrow 0$ , the wave packet can be arbitrarily narrow, i.e.  $v \rightarrow \infty$ , so it can probe the lowest point of the potential well, and we are in the classical regime. The energy density in this limit vanishes.

### 3.3 Equations of Motion

To obtain the semi-classical equations of motion we calculate the expectation value of the time derivative:

$$\langle i\hbar\partial_t \rangle = \sum_l (-\hbar f \dot{w}_l + i f \text{tr}(E_{l0} \dot{U}_{l0} U_{l0}^{-1})). \quad (46)$$

Inserting this expression as well as the one for  $\langle H \rangle$  in (2) and performing the variation, we obtain the equations of motion for each link (the subscript 0 is suppressed and  $f_l$  stands for  $f(v_l)$ ):

$$\begin{aligned} \dot{E}_l^a &= \frac{i}{f_l} \sum_{p(l)} \text{tr}(f_p \tau^a U_p) - \frac{3\hbar w_l}{8 v_l} E_l^a, \\ \dot{U}_l &= \frac{i}{2f_l} \left(1 - \frac{f_l}{2v_l}\right) E_l U_l, \\ \dot{v}_l &= \frac{3\hbar f_l w_l}{8 f_l' v_l}, \\ \dot{w}_l &= \left(\frac{1}{f_l} - \frac{1}{2v_l}\right) E_l^2 + \left(\frac{E_l^2}{4v_l} + \frac{2}{f_l} \sum_{p(l)} f_p \text{tr} U_p - \frac{3}{16} \hbar^2 (v_l + \frac{w_l^2}{v_l})\right), \\ &\quad - \frac{f_l}{f_l'} \left(\frac{E_l^2}{4v_l^2} + \frac{3}{16} \hbar^2 (1 - \frac{w_l^2}{v_l^2})\right), \end{aligned} \quad (47)$$

where  $f_l'$  is the derivative of  $f_l$  with respect to  $v_l$ , the sum over  $p(l)$  runs over all four plaquettes sharing the link  $l$  and  $U_p$  here is the ordered plaquette variable starting with link  $U_l$ . We note that in the limit of small width or large  $v$  the equations assume the correct classical form,

$$\begin{aligned} \dot{E}_l^a &= i \sum_{p(l)} \text{tr}(\tau^a U_p), \\ \dot{U}_l &= i E_l U_l. \end{aligned} \quad (48)$$

Hence the equations (47) can be used to study the quantum corrections to the classical evolution (48). These equations can also be studied in the limit where  $v$  is fixed and  $w = 0$ , where the equations take the form

$$\begin{aligned} \dot{E}_l^a &= \frac{i}{f_l} \sum_{p(l)} \text{tr}(f_p \tau^a U_p), \\ \dot{U}_l &= \frac{i}{2f_l} (1 - \frac{f_l}{2v_l}) E_l U_l. \end{aligned} \quad (49)$$

The fixed width parameter  $v$  is to be treated as a variational parameter.



### 3.4 Classical Limit

In order to be able to define a trajectory in phase space the wave packet must be narrow compared to the total available phase space volume. The restriction comes both from the link variables  $U$  (coordinates) and electric field variables  $E$  (momenta). To have a quantitative measure of how localized the wave packet is, we define a quantity  $\alpha(v)$  which is the ratio of the volume of the wave packet and the total group volume,  $2\pi^2$  for  $SU(2)$ , i.e.:

$$\alpha(v) = (1 - f)^{3/2} \rightarrow \begin{cases} 1 & v \rightarrow 0 \\ \left(\frac{3}{4v}\right)^{3/2} & v \rightarrow \infty. \end{cases} \quad (50)$$

The function  $\alpha(v)$  is shown in Fig.1 (dotted line). If we request  $\alpha(v) < 0.1$ , we need  $v > 5$  and  $\hbar < 1$  for  $T \approx 1$ . The largest distance in momentum space is controlled by excitation energy as  $d_E \sim \sqrt{E}$  or  $d_E \sim T$ . We require  $\Delta E \ll d_E$ . In the classical limit ( $v \rightarrow \infty$ ) this requires  $\hbar \ll T$ , which in the unscaled variables is

$$\frac{\hbar}{Ta} = \frac{k_{max}}{\pi T} \ll 1. \quad (51)$$

where  $k_{max}$  is the largest wave number that is possible to appear on the lattice. Physically this means that we shall only keep the long wavelength modes on the lattice which is consistent to our intuition.

## 4 Results and Discussions

With the above semi-classical equations of motion we can follow a trajectory in the space of gauge fields for every given initial condition. To make the results comparable to those of our calculations for the classical gauge theory, we specify the initial gauge configuration in the same way as in ref.[3]. We initially choose all electric field variables to be zero to satisfy Gauss's law. The magnetic sector is initialized by choosing the link variables  $U_l = \cos(\rho/2) - i\mathbf{n} \cdot \tau \sin(\rho/2)$  randomly and the total energy is varied by selecting  $\delta$  which limits the range of the parameter  $\rho$  to  $(0, 2\pi\delta)$ . In addition here we specify  $\hbar$  and the width parameters. Initially we choose identically on each link  $v = 20$  and  $w = 0$ . The results are given in Table 1.

To present our result we need to specify our controllable parameters. One of these is  $\hbar = 4\pi\alpha_s$ , which is a manifestation of quantum effects. Another should be chosen to give a measure of the excitation energy of the system. A direct comparison between classical and quantal systems with the same energy is unphysical because of the appearance of a zero-point energy in the latter. A convenient comparable parameter is the physical temperature of an excited system. The problem now is how to measure the temperature on the lattice. For a weakly interacting system, we can extract the temperature as follows. The energy distribution for a small subsystem is measured, which factorizes into a phase space prefactor and an exponential  $\exp(-E/T)$ . Dividing out the phase space factor we can simply identify the temperature as the rate of exponential slope of the energy distribution. But here this method cannot be used directly because the lattice gauge system is a constrained and strongly coupled system. This problem will be discussed in detail elsewhere. Here we make the observation that the relative difference between the electric part of the semi-classical Hamiltonian and that of the classical one is  $1/(2v)$  which is very small in the limit of large  $v$ . As a consequence, the value of  $\langle\langle H_e \rangle\rangle$ , the average electric energy per link, at a certain temperature  $T$  of the classical system and that of the semi-classical system in the limit of large  $v$  will be similar. Neglecting the small difference, we can use it as a measure of the excitation level of the system, and define parameter  $T_e \equiv \langle\langle H_e \rangle\rangle$  as the "electric temperature" of the gauge field.

We have measured width parameters on the lattice. The results are shown in Fig.3 for  $\hbar = 0.3$  and  $T_e = 0.9$ , and in Table.1. In Fig.3a and 3b, the time evolution of the average values of  $v$  and  $w$  are shown. The average is taken over the lattice, which is expected to coincide with the ensemble average if the lattice is sufficiently large. We find that these values are quickly damped into their equilibrium positions, which are independent of their initial value. The final distributions of  $v$  and  $w$  over the lattice are shown in Fig.3c and 3d respectively. The imaginary part of the width parameter  $w$  obviously has zero mean value. The nonzero expectation value of  $v$  depends mainly on  $\hbar$  as we can see from column 4 of Table 1. We have obtained the least error fit

$$\langle\langle v \rangle\rangle \approx 7/\hbar. \quad (52)$$

The  $T_e$  dependence is difficult to see because  $T_e$  does not change much between runs. The  $\hbar$  dependence roughly agrees with (44), which is found for the system without constraints and couplings by the standard thermodynamical method.

We have also measured the electric energy distribution which is shown in Fig.4 for the same initial condition as in Fig.3. The histogram is from the simulation. The solid curve is a fit,

$$f(H_e) \sim \sqrt{H_e} \exp(-H_e/0.6), \quad (53)$$

apart from a normalization constant. It has correct mean value  $\langle\langle H_e \rangle\rangle = 0.9$  and looks very much like a Boltzmann distribution. We note that for a constrained system it is possible for the exponential in the energy distribution to have the form  $\exp(-\beta E/T)$  where  $\beta$  can be different from 1. So here we do not conclude the system temperature is 0.6.

Now we come to the question which originally motivated this study, namely, whether the quantum effects suppress or enhance the chaotic behavior of a pure gauge system. For this purpose we shall measure the maximal Lyapunov exponents  $\lambda$  in our semi-classical formalism and compare them with the ones we found for the classical lattice gauge theory at the same  $T_e$ . The logarithmic scale of the divergence of trajectories is shown by the solid line in Fig.5, where  $\hbar = 0.3$  and  $T_e = 0.9$ . For comparison, we also show in the same plot the divergence of two corresponding classical trajectories, with same  $T_e$ , by the dotted line. The distance measure used here is the same as that in ref.[3], i.e., the integrated absolute value of the local difference in magnetic energy. At early times, while the classical evolution smoothly increases the distance between the two trajectories, there is a sudden jump of the distance to a value independent of  $D_0$  in the semi-classical evolution, which originates from the couplings of  $U_l$  and  $E_l$  to the width parameters  $v_l$  and  $w_l$ . The latter oscillate and are damped strongly in the beginning as we see in Fig.3. Also at early times the fluctuations are large on the logarithmic scale compared to the purely classical evolution. These fluctuations are quantum effects. At larger times the exponential increase of the distance emerges from the fluctuating background. We see the rate of exponential growth is larger than that of the classical one. The distance finally reaches a maximum value. The maximal Lyapunov exponent is extracted from the linear region in the plot. Due to the large fluctuations this method is less accurate here than it is in the classical case. The numbers obtained for  $\lambda$  have errors of the order of  $\pm 0.02$ . We performed three runs for the system with the same  $\hbar$  and  $T_e$  and find that the statistical error is dominated by our measuring error. The results for different initial conditions are shown in column 3 of Table.1. At  $\hbar = 0.1$  the result deviates very little from the classical result  $\lambda_c = T_e/3$ . The correction to  $\lambda$  is represented by  $\delta\lambda$  (column 4) which is defined as  $\lambda(T_e, \hbar) = \lambda_c(T_e)(1 + \delta\lambda)$ .  $\delta\lambda$  depends both on  $\hbar$  and  $T_e$ . The relation is not easily extracted from the data due to the lack of accuracy, but we note that the sign of  $\delta$  is always positive. This suggests that quantum corrections enhance the chaoticity of the classical gauge system. The physical implication is that including the quantum corrections, the initial state of the gauge field will thermalize more rapidly.

We have also measured the time dependence of the distance between two trajectories originating from the same point but one evolved with the classical equations and the other with the variational quantum equations. This distance also diverges exponentially, because as soon as the quantum corrections generate deviation between the trajectories the difference will diverge with time because of the chaoticity of our system. This leads to the question whether the trajectory of the centroid of the wave packet has any physical meaning. If we want to describe the quantum corrections to a particular classical trajectory exactly, then the method of Gaussian variational states obviously fails. However, if we are only interested in the ensemble averaged properties of the system, e.g. the rate of the increase of the coarse grained phase space volume, the approach remains useful. This is not too serious a drawback because even in the classical limit we cannot numerically follow the exact evolution of a particular trajectory for a long time, and we have to limit ourselves to the study of average properties of the system.

In conclusion, starting from a Gaussian ansatz we have derived a set of semi-classical equations of motion for the lattice SU(2) gauge field via a variational method. These equations were used to study the quantum corrections to the classical evolution. We find the quantum effects enhance the chaoticity of the gauge field.

*Acknowledgements:* We thank S. G. Martinyan and J. Rau for fruitful discussions. This work was supported in part by the U.S. Department of Energy (Grant No. DE-FG05-90ER40592) and by a computing grant from the North Carolina Supercomputing Center.

## References

- [1] S. G. Matinyan, G. K. Savvidy and N. G. Ter-Arutyunyan-Savvidy, Sov. Phys. JETP **53** (1981) 421; JETP Lett. **34** (1981) 590
- [2] S. G. Matinyan, E. B. Prokhorenko, and G. K. Savvidy, Nucl. Phys. **B298** (1988) 414; Yad. Fiz. **50** (1989) 284 [ Sov. J. Nucl. Phys. **50** (1989) 178]
- [3] B.Müller and A. Trayanov, Phys. Rev. Lett. **68** (1992) 3387; C. Gong, Phys. Lett. **B 298** (1993) 257
- [4] E. Wigner, Phys. Rev. **40** (1932) 749
- [5] J. H. Hannay and M. V. Berry, Physica **D 1** (1980) 267
- [6] S. John and E. A. Remler, Ann. Phys. **180** (1987) 152, and refernces therein
- [7] P. Stevenson, Phys. Rev. **D32** (1985) 1389; T.S. Biró, Ann. Phys. **191** (1989) 1
- [8] P. Kramer, M. Saraceno, Geometry of the Time-dependent Variational Principle in Quantum Mechanics, Lecture Notes in Physics **140**, Springer Verlag 1981
- [9] M. Saraceno, P.Kramer, and F. Fernandez, Nucl. Phys. **A405** (1983) 88
- [10] H. Feldmeier, Nucl. Phys. **A515** (1990) 147
- [11] C. Corianó, R. Parwani and H. Yamagishi, Nucl. Phys. **A522** (1991) 591
- [12] S. A. Chin, O. S. Van Roosmalen, E. A. Umland and S. E. Koonin, Phys. Rev. **D31** (1985) 3201

## Table Captions

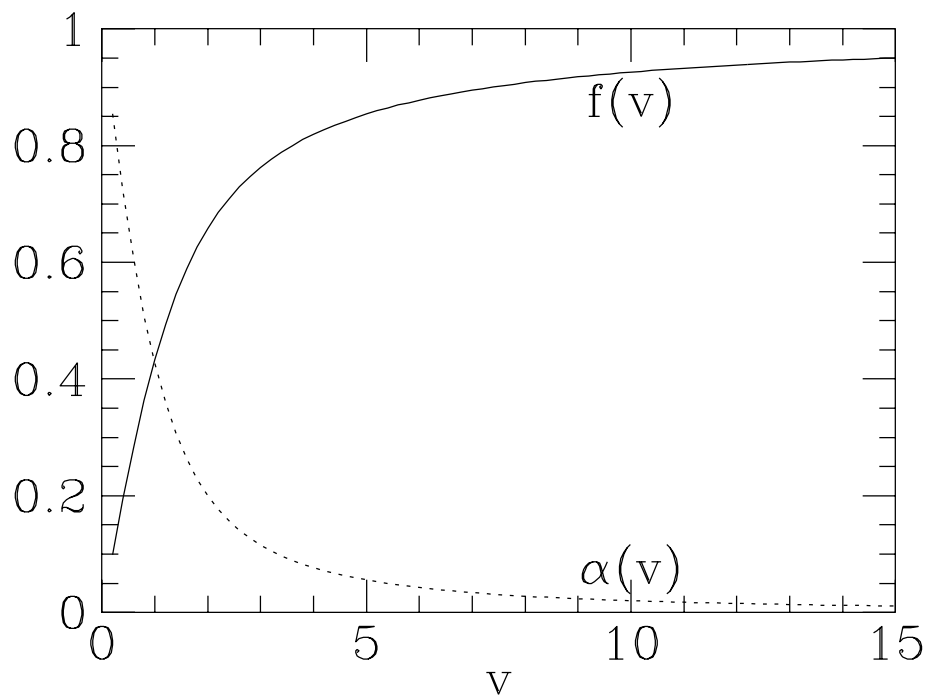
Table.1 Results of numerical simulations.

## Figure Captions

- Fig.1 The solid line shows function  $f(v)$  and the dotted line shows wave packet volume ratio  $C(v)$  as a function of  $v$  .
- Fig.2 Dependence of the free energy on  $v$  for different values of  $\hbar$  at  $T = 0.5$  (a) and  $T = 0$  (b). The solid line is for  $\hbar = 0.1$ , the dotted line is for 1, the short dashed line is for 1.732 and the long dashed line is for  $\hbar = 3$ .  $v \rightarrow \infty$  corresponds to the classical limit of an infinitely narrow wavepacket.
- Fig.3 Width properties for  $T_e = 0.9$  and  $\hbar = 0.3$ : The equilibrium distribution of  $v$  (a) and  $w$  (b) and time evolution of the mean values of  $v$  (c) and  $w$  (d).
- Fig.4 Final electric energy distribution for  $T_e = 0.9$  and  $\hbar = 0.3$ .
- Fig.5 The solid line shows the divergence of the centroids for the two neighbouring Gaussian field configurations for  $T_e = 0.9$  and  $\hbar = 0.3$ . The corresponding divergence for the two classical field configurations with the same  $T_e$  is shown by the dotted line.

Table.1

$\hbar$	$T$	$\lambda$	$\delta\lambda$	$\langle\langle v \rangle\rangle$	$E$
0.1	0.76	0.255	0.01	70	2.13
0.3	0.64	0.24	0.12	23	2.48
0.3	0.73	0.3	0.22	22	2.92
0.3	0.85	0.34	0.2	21	3.31
0.3	0.85	0.36	0.27	21	3.25
0.3	0.85	0.34	0.2	22	3.25
0.3	0.9	0.41	0.37	20	3.74
0.7	0.5	0.19	0.16	9.0	3.24
0.7	0.8	0.41	0.54	7.4	4.40



This figure "fig2-1.png" is available in "png" format from:

<http://arxiv.org/ps/hep-lat/9305024v1>

This figure "fig3-1.png" is available in "png" format from:

<http://arxiv.org/ps/hep-lat/9305024v1>

This figure "fig4-1.png" is available in "png" format from:

<http://arxiv.org/ps/hep-lat/9305024v1>



This figure "fig5-1.png" is available in "png" format from:

<http://arxiv.org/ps/hep-lat/9305024v1>

This figure "fig6-1.png" is available in "png" format from:

<http://arxiv.org/ps/hep-lat/9305024v1>

